ATLAS NOTE

ATLAS-CONF-2013-088

August 15, 2013
Minor revision: September 9, 2013

Preliminary results on the muon reconstruction efficiency, momentum resolution, and momentum scale in ATLAS 2012 pp collision data

The ATLAS collaboration

Abstract

The ATLAS experiment identifies and reconstructs muons with two high precision tracking systems, the Inner Detector and the Muon Spectrometer which provide independent measurements of the muon momentum. This note summarizes the performance of the muon reconstruction algorithms and the data-driven techniques used for the measurements as derived from a dataset corresponding to an integrated luminosity of 20.4 fb^{-1} of 8 TeV pp collisions recorded in 2012. We also describe the corrections to be applied to simulation to reproduce the efficiency, momentum resolution and scale observed in experimental data. Finally, we introduce a method to determine the momentum uncertainty using the muon track fit uncertainty.

Corrected typo in the legend of Figure 10 with respect to the version of August 15, 2013

1 Introduction

Efficient and accurate muon identification and reconstruction is of primary importance for the physics program of the ATLAS experiment [1]. This note describes preliminary results on the muon reconstruction efficiency, momentum resolution, and momentum scale derived from the dataset corresponding to an integrated luminosity of 20.4 fb^{-1} of 8 TeV pp collisions delivered by the Large Hadron Collider (LHC) during the 2012 run.

Section 2 briefly describes the algorithms used for muon identification and reconstruction in the ATLAS experiment. They use the independent track reconstruction provided by two sub-detector systems: the Inner Detector [2] (ID) and the Muon Spectrometer [3] (MS). The combination of the ID and MS information increases the purity of the muon sample and ensures good momentum resolution over three orders of magnitude of muon energy: from a few GeV up to a few TeV.

Section 3 summarizes the characteristics of the selected datasets and of the Monte Carlo samples (MC) used for data-simulation comparisons.

Sections 4 and 5 report the measurements of the muon reconstruction efficiency and momentum resolution. The methodologies used in these measurements, documented in detail in previous publications [4, 5], are based on the reconstruction of $Z \to \mu\mu$ decays in simulated events and in experimental data. The decays of $J/\psi \to \mu\mu$ and $\Upsilon \to \mu\mu$ are also used for validation and for the study of systematic uncertainties.

Finally, Section 6 describes a method that uses the muon track fit uncertainty to evaluate the momentum uncertainties in an independent way.

2 Muon identification and reconstruction

The ATLAS experiment uses the information of the MS and ID sub-detectors, and to a lesser extent, of the calorimeter, to identify and precisely reconstruct muons produced in the pp collisions.

The MS is the largest of all ATLAS sub-detectors: it is designed to detect charged particles in the pseudorapidity[1] region up to $|\eta| = 2.7$ and to provide momentum measurement with a relative resolution better than 3% over a wide p_{T} range and up to 10% at $p_{\mathrm{T}} \approx 1$ TeV. The MS consists of one barrel part (for $|\eta| < 1.05$) and two end-cap sections. A system of magnet coils provides a toroidal magnetic field with a bending integral of about 2.5 Tm in the barrel and up to 6 Tm in the end-caps. Triggering and η, ϕ position measurements, with typical resolution of $5 - 10$ mm, are provided by the Resistive Plate Chambers (RPC, three layers for $|\eta| < 1.05$) and by the Thin Gap Chambers (TGC, three layers for $1.0 < |\eta| < 2.4$). Precision muon momentum measurement in the plane transverse to the beam-pipe is possible up to $|\eta| = 2.7$ and it is provided by three layers of Monitored Drift Tube Chambers (MDT) everywhere except for $|\eta| > 2$ where the innermost MDT layer is replaced by one layer of Catode Strip Chambers (CSC). The single hit resolution in the bending plane for the MDT and the CSC is about 80 μm and 60 μm, respectively.

An independent determination of the muon momentum is provided by the ID. It consists of three sub-detectors: the inner Silicon Pixels and the Semi-Conductor Tracker (SCT) detectors for $|\eta| < 2.5$, and the outer Transition Radiation Tracker (TRT) covering $|\eta| < 2.0$. They provide high-resolution coordinate measurements for track reconstruction inside a solenoidal magnetic field of 2 T.

[1] ATLAS uses a right-handed coordinate system with its origin at the nominal interaction point (IP) in the centre of the detector and the z-axis along the beam pipe. The x-axis points from the IP to the centre of the LHC ring, and the y-axis points upward. Cylindrical coordinates (r, ϕ) are used in the transverse plane, ϕ being the azimuthal angle around the beam pipe. The pseudorapidity and the transverse momentum are defined in terms of the polar angle θ as $\eta = -\ln\tan(\theta/2)$ and $p_{\mathrm{T}} = p\sin\theta$, respectively. The $\eta - \phi$ distance between two particles is defined as $\Delta R = \sqrt{\Delta\eta^2 + \Delta\phi^2}$.

Muon identification is performed according to several reconstruction criteria (leading to different muon "types"), according to the available information from the ID, the MS, and the calorimeter sub-detector systems. The different types are:

- Stand-alone (SA) muons: the muon trajectory is reconstructed only in the MS. The direction of flight and the impact parameter of the muon at the interaction point are determined by extrapolating the MS track back to the point of closest approach to the beam line, taking into account the energy loss of the muon in the calorimeters;
- Combined (CB) muon: track reconstruction is performed independently in the ID and MS, and a combined track is formed from the successful combination of a SA track with an ID track;
- Segment-tagged (ST) muons: a track in the ID is identified as a muon if the track extrapolated to the MS is associated with at least one track segment in the MDT or CSC.
- Calorimeter-tagged (CaloTag) muons: a track in the ID is identified as a muon if the track can be associated to an energy deposit in the calorimeter as expected from a minimum ionizing particle. This type has the lowest purity of all the muon types but it recovers acceptance in the uninstrumented region of the MS. The identification criteria of this muon type are optimized for a region of $|\eta| < 0.1$ and a momentum range of $25 \lesssim p_{\mathrm{T}} \lesssim 100$ GeV.

CB candidates have the highest muon purity. The CB muon reconstruction efficiency is strongly affected by acceptance losses in the MS, mainly in two regions:

- at $\eta \approx 0$, the MS is only partially equipped with muon chambers in order to provide space for services for the ID and the calorimeters;
- in the region ($1.1 < \eta < 1.3$) between the barrel and the end-caps, there are regions in ϕ where only one layer of chambers is traversed by muons in the MS, due to the fact that some of the chambers of that region were not yet installed[2]. Therefore, no SA momentum measurement is available and the CB muon efficiency is decreased.

The reconstruction of the first three muon types (all using the MS information) is performed using two independent and complementary strategies [6] (named "Chains"): the first chain (or "Chain 1") performs a statistical combination of the track parameters of the SA and ID muon tracks using the covariance matrices of both track parameter measurements. The second chain (or "Chain 2") performs a global refit of the muon track using the hits from both the ID and MS sub-detectors. All the figures presented in Sections 4, 5 of this note refer to the Chain 1 reconstruction while the corresponding figures for Chain 2 are shown in Appendix A.

3 Data and Monte Carlo Samples

The results presented in this note are obtained from the analysis of $\sqrt{s} = 8$ TeV pp collision events corresponding to an integrated luminosity of 20.4 fb^{-1} and collected by the ATLAS detector in 2012. Online event selection is performed by a three-level trigger system described in Ref. [7]. Events are accepted for the analyses documented in this note only if the ID and MS detectors were in good data-taking conditions and both solenoidal and toroidal magnet systems were on. The $Z \to \mu\mu$ candidates are selected online by requiring at least one muon candidate with $p_{\mathrm{T}} > 24$ GeV and isolated from other activity in the tracker, while lower di-muon mass candidates are selected online by requiring at least two

[2]The installation of all the muon chambers in this region has been completed during the 2013-2014 LHC shutdown.

muon candidates with $p_{\mathrm{T}} > 6$ GeV and with a reconstructed di-muon invariant mass in a window around the J/ψ or the Υ resonance mass.

In the following, experimental data are compared to MC simulations of signal and background processes. The $J/\psi \to \mu\mu$ and $\Upsilon \to \mu\mu$ signal MCs are generated with PYTHIA [8], while the $Z \to \mu\mu$ signal MC is generated with POWHEG [9]. The generated signal events are passed through the full Geant4 [10] simulation of the ATLAS detector, the trigger simulation and the same reconstruction chain used for data. The samples used for background simulation are described in detail in Refs. [4, 5], they include, depending on the case, $Z \to \tau\tau$, $W \to \mu\nu$, $W \to \tau\nu$, $b\bar{b}$, $c\bar{c}$, and $t\bar{t}$ production and decays.

The simulation includes a realistic evaluation of the MS detector misalignment obtained by studying straight muon tracks from cosmic ray events [11] and from special runs performed with the toroidal magnetic field off [12]. When the effect of the realistic misalignment is taken into account the momentum resolution for muons of 1 TeV of energy reaches approximately 13% in the barrel region of the MS, 17% in the end-cap region of the MS, and 15% in the region covered by the CSC sub-detector.

4 Muon reconstruction efficiency

As the track reconstruction in the ID and MS are performed independently, the reconstruction efficiency of the different muon types can be decomposed in the product of the reconstruction efficiency in the ID, the reconstruction efficiency in the MS, and the matching efficiency between the ID and MS measurements (which includes the refit efficiency in the case of Chain 2).

A tag-and-probe method, described in detail in Ref. [4], is employed to measure the reconstruction efficiencies[3] of all muon types within the acceptance of the ID ($|\eta| < 2.5$). As discussed below, the method is sensitive to the quantities of interest, i.e. the ID reconstruction efficiency, and the MS reconstruction efficiency together with the matching efficiency. For $Z \to \mu\mu$ decays, events are selected by requiring two oppositely charged isolated muons[4] with $p_T > 20$ GeV and a di-muon invariant mass within 10 GeV from the Z-boson mass. One of the muons is required to be a CB muon, and to have triggered the readout of the event. This muon is called the "tag". The other muon, the so-called "probe", is required to be a "MS track" (i.e. a SA or a CB muon) when the ID or CaloTag muon efficiencies are to be measured. CaloTag muons are used as probes when the MS reconstruction efficiency together with the matching efficiency is to be measured. The use of CaloTag muons instead of ID track probes as done in Ref. [4] reduces the background in the $Z \to \mu\mu$ sample by an order of magnitude without biasing the efficiency measurement. A total of more than 10^7 data events are selected for the tag-and-probe studies.

After selecting all tag-and-probe pairs an attempt is made to match the probe to the reconstructed muons in the event: a match is successful when the muon and the probe have the same measured charge and they are close in the $\eta - \phi$ plane ($\Delta R < 0.01$ for ID probes, $\Delta R < 0.05$ for MS probes). For each muon reconstruction type the equation of the reconstruction efficiency is:

$$\varepsilon(\text{Type}) = \varepsilon(\text{Type}|\text{ID}) \cdot \varepsilon(\text{ID}) \quad \text{with Type} = \text{CB, ST,} \tag{1}$$

where ε(Type|ID) is the MS reconstruction and the matching efficiency for a specific muon type measured with CaloTag probes, and ε(ID) is the ID reconstruction efficiency which is the fraction of MS track probes associated to an ID track.

The level of agreement of the measured muon efficiencies ε^{Data} with the efficiencies ε^{MC} predicted by the MC simulation is expressed as the ratio between these two numbers, further on called "efficiency

[3] Efficiencies determined with the tag-and-probe method, and with an alternate method based on MC truth, were found to agree within statistical uncertainty [6, p.221]. This also shows that any possible correlations between the tag and the probe muons are negligible.

[4] In the rest of this note a muon is considered to be isolated when the sum of the momenta of the tracks with $p_T > 1$ GeV detected in a cone of $\Delta R = 0.4$ around the muon track is less than 0.1 times the muon momentum itself.

scale factor" or SF:

$$SF = \frac{\varepsilon^{Data}}{\varepsilon^{MC}} \,. \tag{2}$$

The sample of selected tag-and-probe pairs has a very high purity and consists of $Z \to \mu\mu$ decays to a level of more than 99.9%. Previous studies [13, 4] showed that a systematic uncertainty of 0.2% on the efficiency SF value is associated to the uncertainty on the evaluation of the residual background contamination and to the comparison of the SF extraction using CaloTag or ID track probes. Another source of systematic uncertainty derives from the measurement of the muon reconstruction efficiency for muons with lower momenta. This was studied in 2010 with $J/\psi \to \mu\mu$ decays [14]. The efficiency measurements of muons with $p_{\mathrm{T}} > 10$ GeV from J/ψ decays were found to agree (within uncertainties) with the efficiency measurements of muons from $Z \to \mu\mu$ decays. A deviation of the SFs up to 2% was found for lower momenta. Hence, as done in Ref. [4], the SF derived from $Z \to \mu\mu$ decays is used also for lower momenta but a systematic uncertainty of 1% is used for $7 < p_{\mathrm{T}} < 10$ GeV whereas 2% uncertainty is assigned for $p_{\mathrm{T}} < 7$ GeV.

The third source of systematic uncertainty is related to the use of the SFs for muons with transverse momenta beyond the range covered by this efficiency measurement. As shown in the rest of the section, the measured SFs do not depend on the transverse momentum of the muons in the range considered. An upper limit on the SF variation for muon momentum of 1 TeV has been extracted by using a MC simulation with built-in imperfections, like a realistic residual misalignment of the detector components or a 10% variation of the muon energy loss. On the basis of this analysis a systematic uncertainty of $1\% \times p$, with p in TeV, is added for $p_{\mathrm{T}} > 100$ GeV.

The very large sample of $Z \to \mu\mu$ decays recorded in the 2012 data taking period allows also the study of the reconstruction efficiency with very fine binning in several variables of interest in order to derive corrections for small discrepancies between data and simulation.

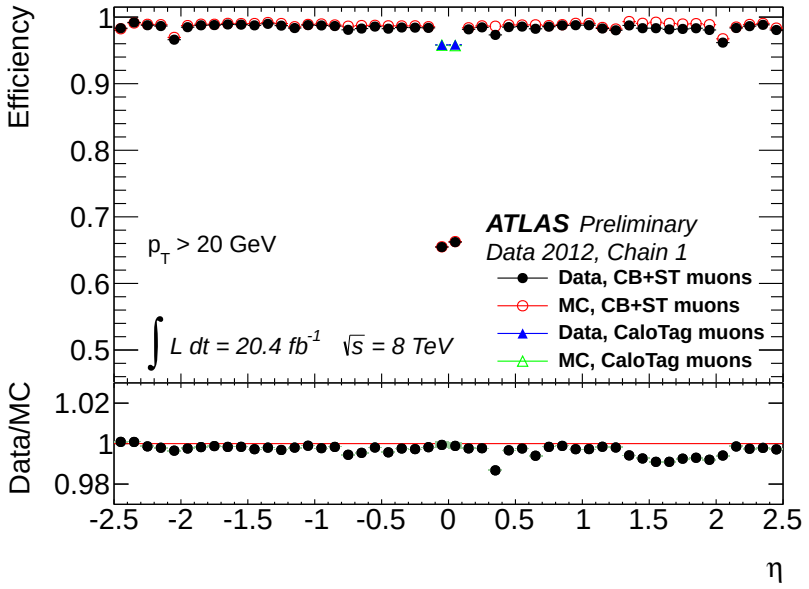

Figure 1: Muon reconstruction efficiency as a function of η for muons with $p_{\mathrm{T}} > 20$ GeV and different muon reconstruction types. CB and ST muon types are reconstructed using the Chain 1 reconstruction algorithm. CaloTag muons are used only in the region $|\eta| < 0.1$. The panel at the bottom shows the ratio between the measured and predicted efficiencies.

Figure 1 shows the muon reconstruction efficiency as a function of η. The combination of all the muon reconstruction types (for CB, ST, and CaloTag muons) gives a uniform muon reconstruction efficiency of about 0.98 over all the detector regions. The inefficiency of the CB+ST muons at $\eta \approx 0$ is almost fully recovered by the use of CaloTag muons. The efficiencies measured in experimental and simulated data are in good agreement (within 0.5%) apart from the region at $1.5 \lesssim \eta \lesssim 2.2$. This behaviour originates from a mis-modeling of the ID reconstruction efficiency that will be discussed below.

The ID muon reconstruction efficiency for $p_{\mathrm{T}} > 20$ GeV as a function of η is analysed in Figure 2: the left part of the figure shows an efficiency greater than 0.99, apart from the regions around $\eta = 0$ and $|\eta| = 1.7$. Figure 2, on the right, shows the ID muon reconstruction efficiency when only minimal ID track identification requirements (described in Ref. [15]) are applied on the muon track. The additional requirement of one hit in the innermost pixel detector layer is applied to muons passing through a sensitive area of this detector in order to ensure an accurate impact parameter measurement. The fact that not all non-operating pixel modules were treated as insensitive regions at the time of the muon reconstruction causes an inefficiency in experimental data at $1.5 \lesssim \eta \lesssim 2.2$ not modeled in simulation.

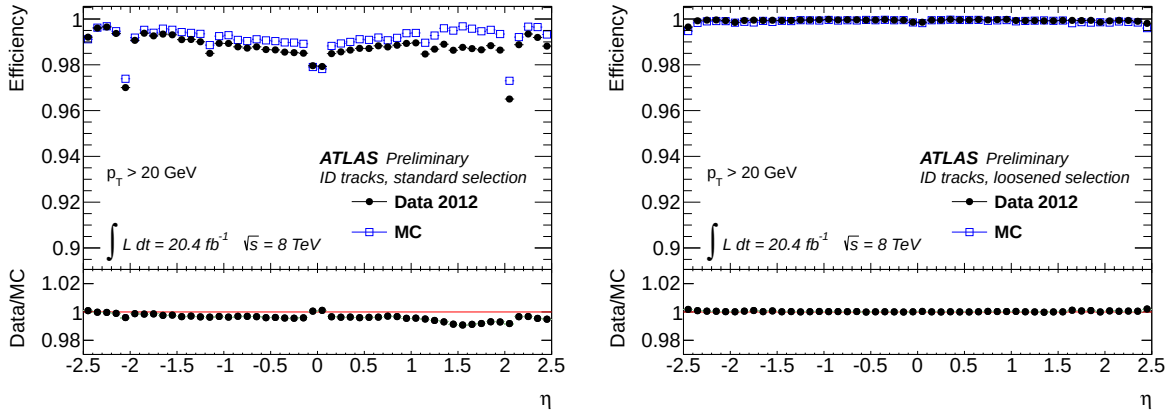

Figure 2: Measured ID muon reconstruction efficiency as a function of η for muons with $p_{\mathrm{T}} > 20$ GeV. On the left plot the efficiency is calculated with the standard selection requirements on the hit multiplicity in the ID while the requirements are relaxed on the right plot. The panel at the bottom shows the ratio between the measured and predicted efficiencies.

A further break down of the results into the CB and CB+ST categories is shown in Figure 3. The CB efficiencies are significantly lower than 0.95 in the partially instrumented regions of the MS at $\eta \approx 0$ and in the poorly instrumented MS region at $\eta \approx 1.2$. The origin of the deviation of the SFs from 1 at $|\eta| \approx 1.2$ and $|\eta| \approx 1.0$ is under investigation. A higher efficiency is achieved when ST muons are added to CB muons.

The CB and CB+ST reconstruction efficiencies are predicted to be independent of the transverse momentum of the muon in the p_{T} range under consideration which is confirmed by the experimental results as shown in Figure 4. The CaloTag muon efficiency is also well predicted by the MC simulation reaching a plateau efficiency of approximately 0.97 for $p_{\mathrm{T}} \gtrsim 30$ GeV.

Figure 5 shows the reconstruction efficiency for CB+ST muons as a function of the average number of inelastic pp interactions per bunch crossing (the $\langle\mu\rangle$ parameter) displaying a high value (on average above 0.97) and remarkable stability. A small efficiency drop of about 2% is only observed for $\langle\mu\rangle \gtrsim 35$ mainly caused by a decrease in the ID reconstruction efficiency. The discrepancy in the data/MC ratio is due to the additional requirement of one hit in the innermost pixel detector layer (for muons passing through a sensitive area of this detector) as discussed above.

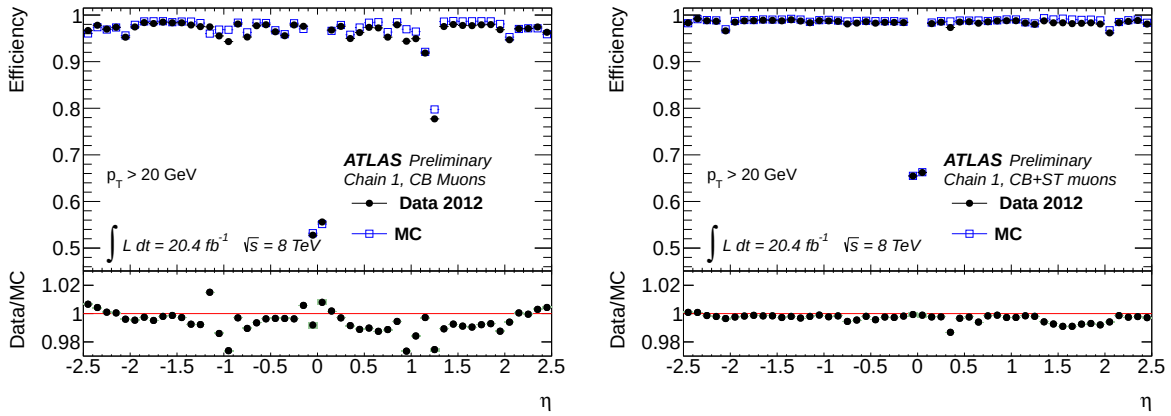

Figure 3: Reconstruction efficiency for Chain 1 CB only muons (left) and CB+ST muons (right) as a function of η for muons with $p_{\mathrm{T}} > 20$ GeV. The panel at the bottom shows the ratio between the measured and predicted efficiencies.

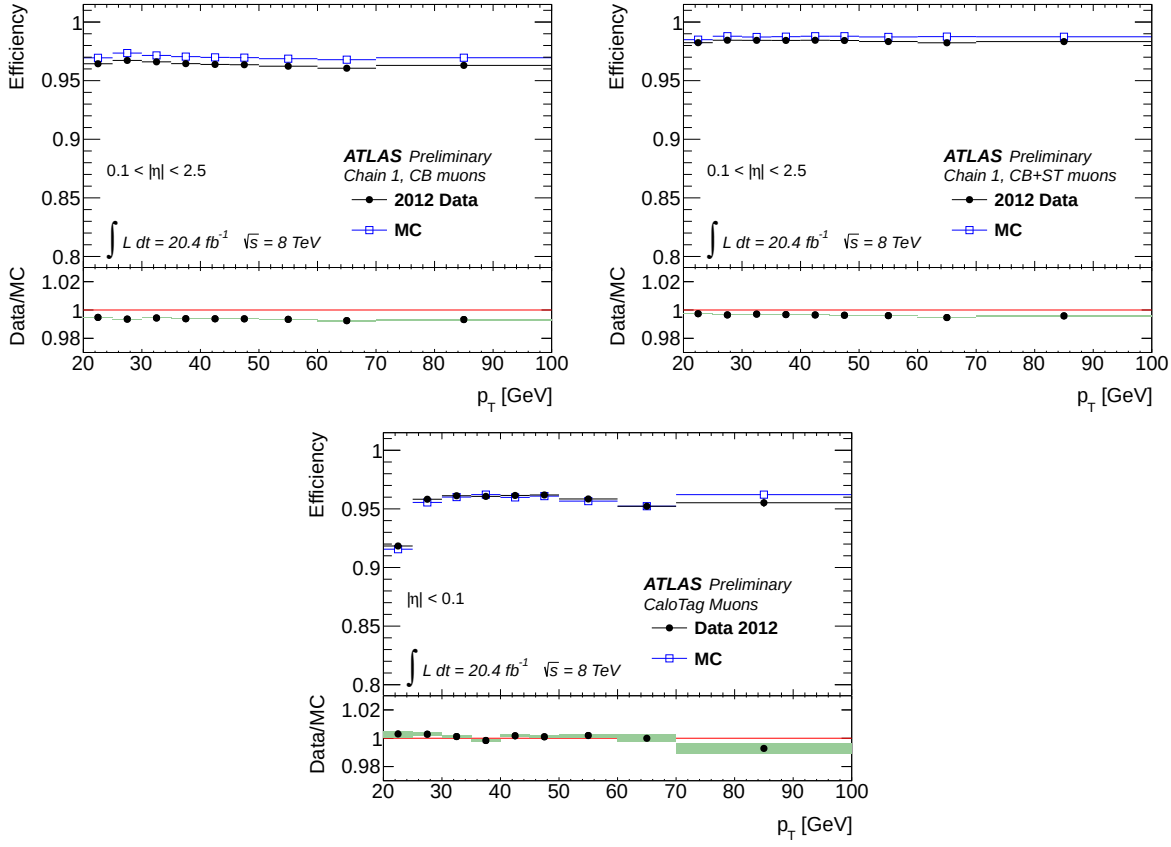

Figure 4: Reconstruction efficiency for Chain 1 CB only muons (top left) and CB+ST muons (top right) as well as CaloTag muons (bottom) as a function of the p_{T} of the muon for muons with $0.1 < |\eta| < 2.5$ for Chain 1 and $0 < |\eta| < 0.1$ for CaloTag muons. The panel at the bottom shows the ratio between the measured and predicted efficiencies.

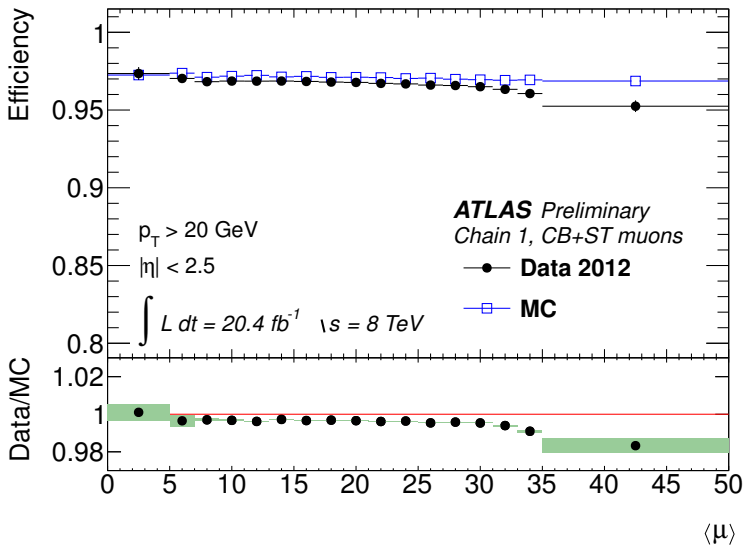

Figure 5: Measured CB+ST (Chain 1) muon reconstruction efficiency for muons with $p_{\mathrm{T}} > 20$ GeV as a function of the average number of inelastic pp collisions per bunch crossing (the $\langle\mu\rangle$ parameter). The panel at the bottom shows the ratio between the measured and predicted efficiencies.

5 Muon momentum scale and resolution

The momentum resolution and scale are additional important parameters used in the evaluation of the muon reconstruction performance. Di-muon decays of the Z, J/ψ, and Υ resonances are used to determine the muon momentum resolution and scale. This allows a validation of the MC prediction for these quantities.

The basic algorithm used in this measurement is described in detail in Ref. [5]. Due to the very large data sample collected in 2012, several improvements of the original method have been made during the analysis of this dataset. A $Z \to \mu\mu$ sample of more than $5 \cdot 10^6$ data events is selected by requiring two isolated CB muons of opposite charge, $p_{\mathrm{T}} > 25$ GeV, and with a reconstructed invariant mass in a window of ± 15 GeV around the Z-boson mass. This gives a very pure sample where the background fraction, estimated using MC simulation, is of the order of 0.1%. The left part of Figure 6 shows that the measured $Z \to \mu\mu$ mass spectrum for the experimental data has a slight shift and a larger spread with respect to the simulated one, obtained with $Z \to \mu\mu$ POWHEG [9] event simulation plus MC background for non-$Z \to \mu\mu$ events.

As reported in Ref. [5], the muon fractional momentum resolution $\frac{\sigma(p_{\mathrm{T}})}{p_{\mathrm{T}}}$, for $p_{\mathrm{T}} > 20$ GeV, can be parametrized to good approximation by the quadratic sum of two terms:

$$\frac{\sigma(p_{\mathrm{T}})}{p_{\mathrm{T}}} = a \oplus b \cdot p_{\mathrm{T}}, \tag{3}$$

where the first term, constant in p_{T}, describes the multiple scattering contribution whilst the second term, proportional to p_{T}, describes the intrinsic resolution caused by the spatial resolution of the detector components, and any residual misalignment. Consequently, the correction to the simulated resolution can also be parametrized by two terms: the first, constant in p_{T}, corrects the multiple scattering contribution while the second, linear in p_{T}, corrects the intrinsic resolution. Finally, if also a momentum scale correction, s, is considered, one arrives to an equation[5] that can be used to derive a corrected momentum

[5]Equation 4 is an approximation, valid in the typical p_{T} range of muons originating from $Z \to \mu\mu$ decays, of the momentum

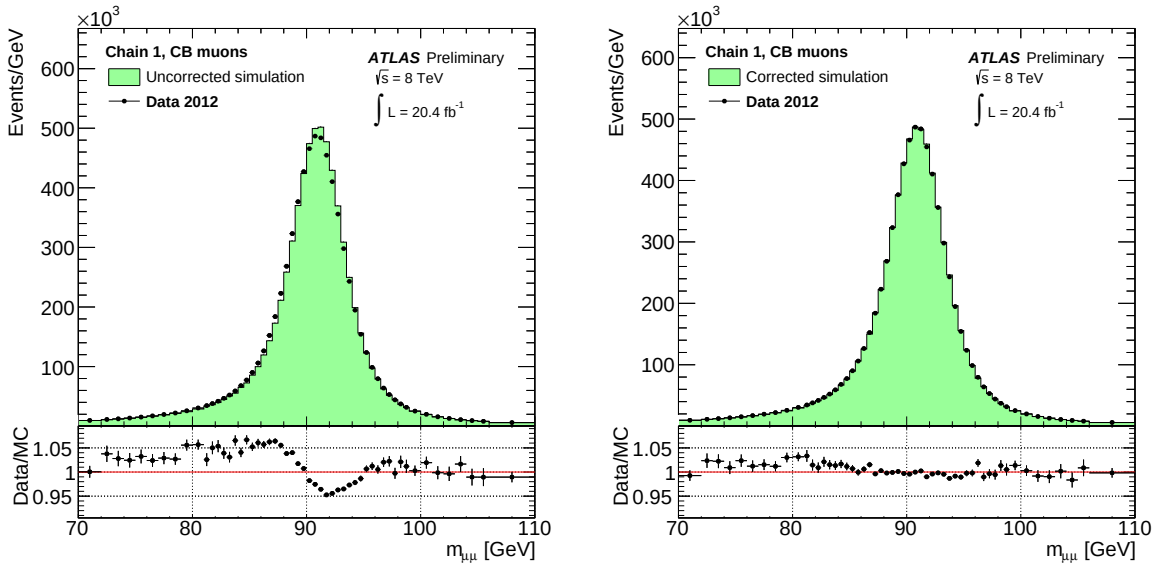

Figure 6: Di-muon invariant mass for Chain 1, CB muons, isolated and with $p_{\mathrm{T}} > 25$ GeV. The plot shows the invariant mass for 2012 data and for the POWHEG [9] simulation of $Z \to \mu\mu$ plus background events. No corrections are applied on the left plot while smearing and scale corrections are applied to the plot on the right. The corrections have been derived from the full 2012 dataset.

measurement, p_{T}^{Cor}, from the simulated momentum measurement, p_{T}^{MC}, with an improved agreement with the one measured in data in the ID and in the MS sub-detectors:

$$p_{\mathrm{T}}^{Cor,det} = p_{T}^{MC,det} \cdot s^{det}(\eta)\left(1 + \Delta a^{det}(\eta)\, G(0,1) + \Delta b^{det}\, G(0,1)\, p_{\mathrm{T}}^{MC,det}\right) \quad \text{with } det = \mathrm{MS, ID}, \tag{4}$$

$G(0,1)$ is a normally distributed random variable with mean 0 and width 1, and the correction factors $s^{det}(\eta)$, $\Delta a^{det}(\eta)$ and $\Delta b^{det}(\eta)$ are derived in 16 different η regions of the detector. The correction of the CB muon momentum is computed as the average of the ID and MS momentum correction weighted by the inverse square of the ID and MS muon momentum resolutions.

The correction parameters are obtained using a MC template fitting technique: a series of mass spectrum distributions is derived from the $Z \to \mu\mu$ simulation by applying Equation 4 with varied correction parameters. Then a binned likelihood fit is used to match the best template to the data mass spectrum. The procedure is iterated across 16 η bins of the detector: the first fit is performed with $Z \to \mu\mu$ events reconstructed with both muons in the same η bin, while the following fits allow also one of the muons in a previously analysed η bin. After all the detector η bins have been analysed, the fit is iterated twice in order to improve the stability of the results.

Figure 7 shows the derived Δa^{MS} and Δb^{ID} resolution correction terms. The main systematic uncertainty derives from the extraction of the corrections from a template fit with a varied window around the Z-boson mass. The two remaining resolution correction terms, i.e. Δa^{ID} and Δb^{MS}, are not extracted from the fit but they are set to zero and varied within the range allowed by systematic uncertainties, as described in Ref. [5]. This procedure is possible because independent measurements constrain Δa^{ID} and Δb^{MS} to be small. The measurement of the material budget in the ID, studied in Ref. [16, 17], is used to predict precisely the contribution of the multiple scattering of muons in the ID, therefore a small Δa^{ID}

resolution correction to be applied to Equation 3. The correction available for physics analyses, which can also probe higher momentum ranges, allows the direct correction of the $1/p_{\mathrm{T}}$ quantity.

term is expected. The effect of the residual misalignment of MS detector components, giving an effective Δb^{MS} term, has been included in the simulation thanks to the studies reported in Section 3.

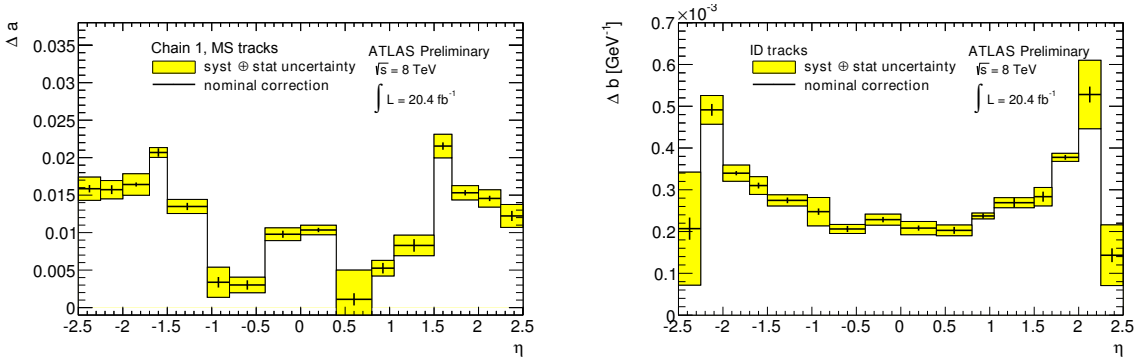

Figure 7: Δa resolution correction term for the MS (left plot), and Δb resolution correction term for the ID (right plot) for MC, derived from $Z \to \mu\mu$ data for the Chain 1 reconstruction. The systematic uncertainty on the correction is shown in yellow.

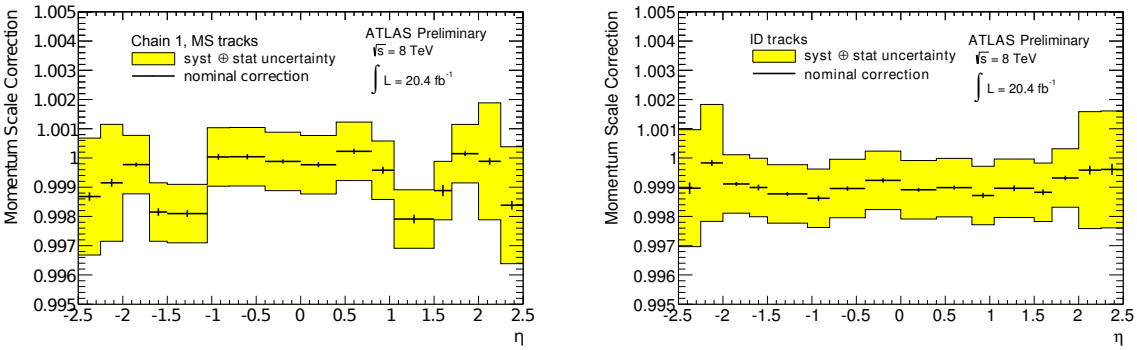

Figure 8: MS (left plot) and ID (right plot) momentum scale correction, for MC, derived from $Z \to \mu\mu$ data for the Chain 1 reconstruction. The systematic uncertainty on the correction is shown in yellow.

Figure 8 shows the derived scale corrections s^{MS} and s^{ID}. Here, the main systematic uncertainties of 0.1% and 0.2% (the second in the forward region of the detector) were introduced to cover a possible momentum dependence of the correction. Figure 9 shows the comparison of the scale obtained at the Z resonance with the Data/MC ratio of the reconstructed mass for lower mass di-muon resonances, J/ψ selected with $p_{\mathrm{T}} > 6$ GeV and Υ selected with $p_{\mathrm{T}} > 6.5$ GeV. The data to MC mass ratio for the $Z \to \mu\mu$ events is obtained with the method described in Section 6 while for $J/\psi \to \mu\mu$ and $\Upsilon \to \mu\mu$ events the mass ratio is obtained with a Gaussian fit of the peak position in data and in MC.

The study shows that there is only a small dependence of the muon momentum scale on the muon momentum. This is caused by the residual inaccuracy of the energy loss correction applied to the MS stand-alone muon momentum measurement. The effect, visible only at small momenta, is covered by the applied systematic uncertainty. A charge dependent effect on the scale corrections has been also investigated and it was found to be covered by the present systematic uncertainty.

The right part of Figure 6 shows the improved agreement between data and MC in the $Z \to \mu\mu$ mass spectrum reconstructed with CB, Chain 1 muons, after the application of the smearing and scale

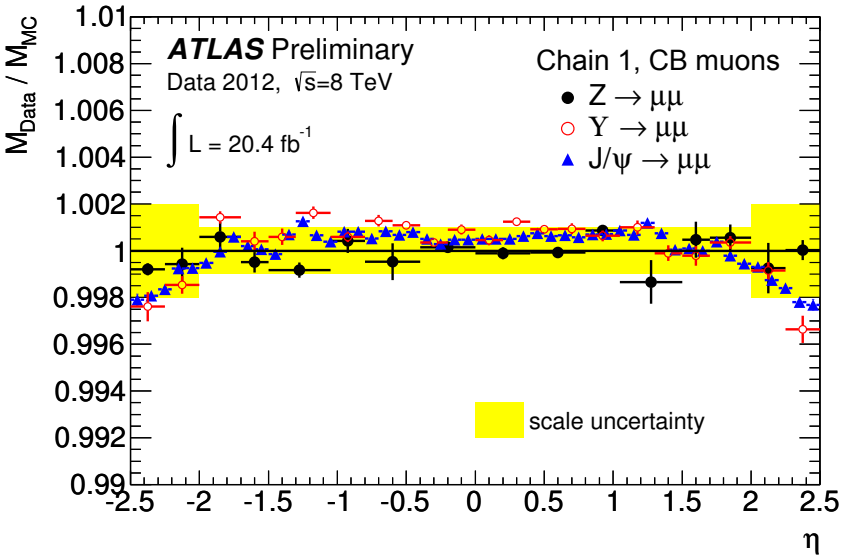

Figure 9: Comparison of the data to MC mass ratio as a function of η for the di-muon decays of Z, J/ψ, and Υ resonances. Selected Z events require two CB muons with $p_{\mathrm{T}} > 25$ GeV and same η bin, selected Υ events require two CB muons of $p_{\mathrm{T}} > 6.5$ GeV and same η bin, selected J/ψ events require two CB muons of $p_{\mathrm{T}} > 6$ GeV and the η of the leading muon is shown. The data to MC mass ratio for the $Z \to \mu\mu$ events is obtained with the method described in Section 6 while for $J/\psi \to \mu\mu$ and $\Upsilon \to \mu\mu$ events the mass ratio is obtained with a Gaussian fit of the peak position in data and in MC.

corrections. The di-muon mass resolution for data and for the uncorrected and corrected simulation is shown in Figure 10: at the Z mass the total Chain 1 CB resolution ranges from 1.5 to 3 GeV in the different detector regions.

6 Validation of the momentum uncertainty estimate of the track fit

In this section we describe an alternative method for addressing the muon momentum resolution and scale that uses the muon track fit uncertainty, $\sigma_{q/p}$, as a per-muon momentum uncertainty function.

The muon momentum resolution can be estimated from the shape of the minimum of the χ^2 minimized by the track fit for each individual muon track. In the χ^2 of the track fit the uncertainties in the positions of the individual components of ID and MS tracking detectors are only treated in an approximate way. This approximate treatment of alignment uncertainties makes it necessary to apply uncertainty scale factors to the momentum uncertainties from the track fit to obtain the correct momentum resolution.

MC simulation studies show that the inverse of the reconstructed muon momentum $1/p_{rec}$ is Gaussian distributed around the true inverse muon momentum $1/p_{gen}$ to good approximation. In order to correct for systematic shifts of p_{rec} with respect to p_{gen} and for an underestimation of the inverse momentum resolution $\sigma_{q/p}$, a momentum scale factor $\alpha(\eta)$ and a resolution scale factor $\beta(\eta)$ are introduced. This leads to a response function of the form:

$$T\left(1/p_{rec}, 1/p_{gen}\right) \equiv \frac{1}{\sqrt{2\pi}\beta(\eta)\sigma_{q/p}} \exp\left[-\frac{\left(\frac{1}{p_{rec}} - \frac{1}{\alpha(\eta)p_{gen}}\right)^2}{2\left(\beta(\eta)\sigma_{q/p}\right)^2}\right], \tag{5}$$

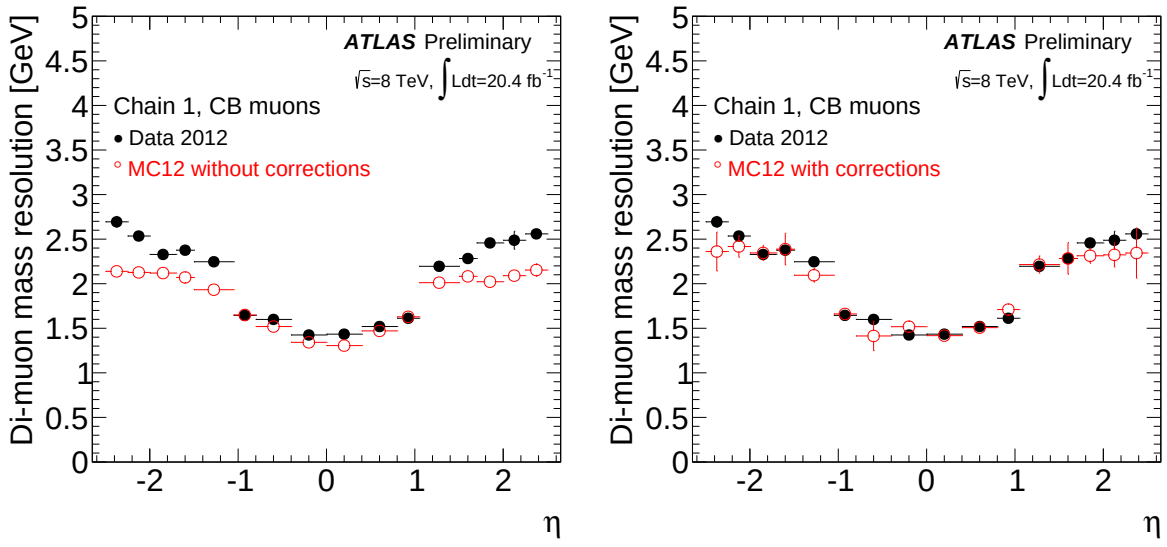

Figure 10: Di-muon mass resolution measured as described in Section 6 for data (black points) and for the uncorrected (left, red points) and corrected (right, red points) simulation for Chain 1 CB reconstructed muons at the Z mass. The two muons are required to be in the same η interval which is indicated in the plot by the horizontal error bars.

where $\alpha(\eta)$ and $\beta(\eta)$ are derived from data and parametrized in pseudorapidity bins.

Due to the good momentum resolution, also the measured mass of a given muon pair $m_{\mu\mu}$ is Gaussian distributed around its true value[6], m_{gen}, to good approximation. As the muon momentum resolution depends on η, ϕ, and p_{T} of a muon, the mass resolution $\sigma_{m_{\mu\mu}}$ is not a constant, but varies from event to event according to the configuration of the muons in $\eta - \phi - p_{\mathrm{T}}$ space. Therefore the di-muon mass resolution is a superposition of Gaussian distributions with different variances $\sigma^2_{m_{\mu\mu}}$. Assuming the two muons to be in the same pseudorapidity interval, the mass response function can be written as

$$T\left(m_{\mu\mu}, m_{gen}\right) \equiv \int_0^\infty f(\sigma^2_{m_{\mu\mu}}) \cdot \frac{1}{\sqrt{2\pi}\beta(\eta)\sigma_{m_{\mu\mu}}} exp\left[-\frac{\left(m_{\mu\mu} - \alpha(\eta)m_{gen}\right)^2}{2\sigma^2_{m_{\mu\mu}}\beta(\eta)^2}\right] d\sigma^2_{m_{\mu\mu}} \tag{6}$$

where $\sigma_{m_{\mu\mu}}$ is the di-muon mass resolution computed with the track fit uncertainties and $f(\sigma^2_{m_{\mu\mu}})$ the probability density function of the mass variances.

A fit of the di-muon mass spectrum in $Z \to \mu\mu$ events with a convolution of the generated mass spectrum and the di-muon resolution of Equation 6 allows the extraction of the $\alpha(\eta)$ and $\beta(\eta)$ parameters and the calibration of the response function. The fit is performed in bins of pseudorapidity by requiring the reconstruction of two CB muons in the same η bin and with a di-muon invariant mass in a window of [85 GeV, 97 GeV]. Studies on simulated data show that the mass scale factor $\alpha(\eta)$ of Equation (6) provided by the fit agrees with the muon momentum scale factor $\alpha(\eta)$ of Equation (5) at the level of 0.05% which is significantly larger than the statistical uncertainty on $\alpha(\eta)$. According to these studies the mass resolution scale factor $\beta(\eta)$ of Equation (6) agrees with the muon momentum resolution scale factor $\beta(\eta)$ of Equation (5) at the level of 3% which is also significantly larger than the statistical error on $\beta(\eta)$. From now on a relative error of 0.05% is assigned to the fit result for $\alpha(\eta)$ and a relative error of 3% to the fit results for $\beta(\eta)$. Repeating the fits in alternative mass windows of [87 GeV, 96 GeV] and

[6] m_{gen} is computed from the four-momenta of the muon pair after final state radiation.

[83 GeV, 99 GeV] leads to values of $\alpha(\eta)$ and $\beta(\eta)$ matching the values from the initial fit within these errors.

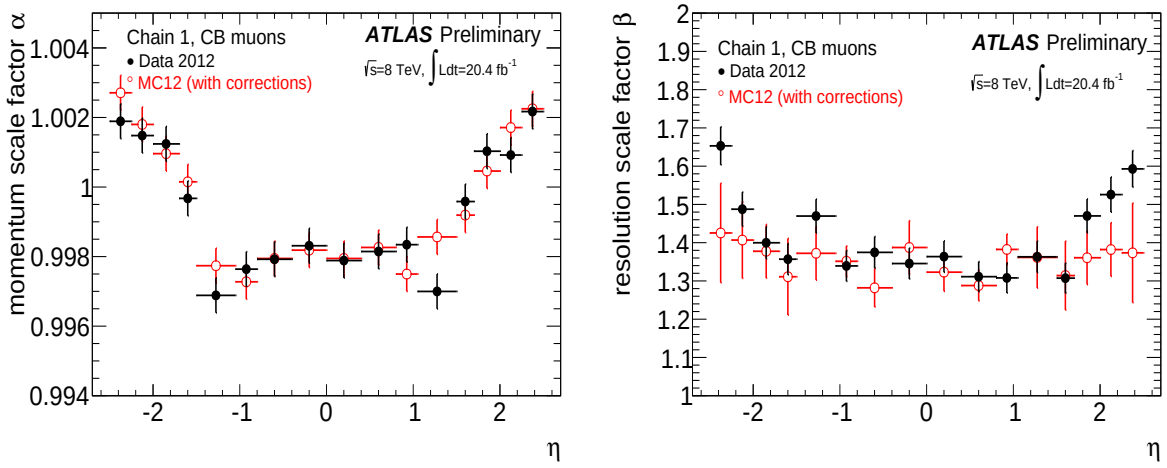

Figure 11: Dependence of the momentum scale factor α (on the left) and of the momentum resolution scale factor β (on the right) on the pseudorapidity of the muon as obtained with the fit described in Section 6. The horizontal error bars represent the size of the pseudorapidity intervals; the vertical error bars shows the total uncertainties on the scale factors. The values have been derived from experimental $Z \to \mu\mu$ data (black points) and for the $Z \to \mu\mu$ POWHEG [9] simulation (red points). The errors of the $\beta(\eta)$ values for the corrected MC sample include the uncertainties of the momentum corrections described in Section 5, they are the dominant contribution to the error bars for $|\eta| > 2.0$.

Figure 11 shows the comparison of the correction factors $\alpha(\eta)$ and $\beta(\eta)$ extracted from experimental data and from the simulation after the application of the corrections of Section 5. The errors of the $\beta(\eta)$ values for the corrected MC sample include the uncertainties of the momentum corrections described in Section 5, they are the dominant contribution to the error bars for $|\eta| > 2.0$. The experimental and simulated data agree within the quoted uncertainties providing an independent validation of both the correction parameters derived in Section 5 and the assumptions of the per-muon momentum error calibrations.

The calibration of the track fit uncertainty $\sigma_{q/p}$, due to the $\beta(\eta)$ parameter, allows the derivation of the di-muon mass resolution in a straightforward way. For each event the corrected $\sigma_{q/p}$ is used to compute a di-muon mass resolution $\sigma_{m_{\mu\mu}}$, the average di-muon mass resolution is defined as the square root of the mean of $\sigma^2_{q/p}$. Figure 10 shows the average di-muon mass resolution as a function of the η of the decay muons for experimental and simulated data. It illustrates the need for muon momentum corrections to match the simulated di-muon mass resolution with the experimentally measured resolution.

7 Summary

This note summarizes the performance of muon identification and reconstruction algorithms used in the ATLAS experiment, the reconstruction efficiency and muon momentum resolution and scale achieved in the 20.4 fb^{-1} dataset of 8 TeV pp collisions recorded during 2012.

The muon reconstruction efficiency is measured to be greater than 0.98, stable against the average number of interactions per bunch crossing and uniform across the detector. The comparison of the reconstruction efficiency in data and in simulation shows good agreement and provides the possibility to

derive efficiency corrections to the simulated muon efficiency in regions of small data/MC disagreement.

The analysis of the $Z \to \mu\mu$ decay mass spectrum is used to measure the muon momentum resolution and scale. The di-muon mass resolution ranges from 1.5 to 3 GeV at the Z mass in the different detector regions. A smearing correction is derived to match the simulated resolution to the data. The muon momentum scale measured in the ID and in the MS is corrected by approximately 0.1%.

A Appendix

This section reports the values of muon reconstruction efficiency and muon momentum corrections for the Chain 2 muon reconstruction algorithm introduced in Section 2. The techniques used in the extraction of the values have been described in Sections 4 and 5, only the noticeable differences are reported in the following.

In particular the comparison of Figure 3 (left plot) with the top right plot of Figure 12 shows that there is no efficiency loss at $\eta \approx 1.2$ for the Chain 2 CB muon reconstruction. This is caused by the fact that the CB muon reconstruction in Chain 2 also accepts MS tracks with poor momentum measurements.

The comparison of the left plot in Figure 13 shows slightly larger correction values for the Δa resolution term of the MS for the Chain 2 muons if compared to the left part of Figure 7; however no appreciable resolution difference appears. Figure 14 shows the $Z \to \mu\mu$ mass spectrum reconstructed with CB, Chain 2 muons (isolated and with $p_{\mathrm{T}} > 25$ GeV), for data and simulation before and after the smearing and scale corrections.

References

[1] ATLAS Collaboration, The ATLAS Experiment at the CERN Large Hadron Collider, JINST 3 (2008) S08003.

[2] ATLAS Collaboration, The ATLAS Inner Detector commissioning and calibration, Eur.Phys.J. C 70, (2010) 787.

[3] ATLAS Collaboration, Commissioning of the ATLAS Muon Spectrometer with Cosmic Rays, Eur.Phys.J. C 70, (2010) 875.

[4] ATLAS Collaboration, Muon reconstruction efficiency in reprocessed 2010 LHC proton-proton collision data recorded with the ATLAS detector, ATLAS-CONF-2011-063 (2011). https://cds.cern.ch/record/1345743

[5] ATLAS Collaboration, Muon Momentum Resolution in First Pass Reconstruction of pp Collision Data Recorded by ATLAS in 2010, ATLAS-CONF-2011-046 (2011). https://cds.cern.ch/record/1338575

[6] ATLAS Collaboration, Expected Performance of the ATLAS Experiment - Detector, Trigger and Physics, CERN-OPEN-2008-020 (2009) 165, arXiv:0901.0512 [hep-ex].

[7] ATLAS Collaboration, Performance of the ATLAS Muon Trigger in 2011, ATLAS-CONF-2012-099 (2012). https://cds.cern.ch/record/1462601

[8] T. Sjöstrand et al., A Brief Introduction to PYTHIA 8.1, Comput. Phys. Comm. 178 (2008) 852, arXiv:0710.3820 [hep-ph].

[9] S. Alioli et al., A general framework for implementing NLO calculations in shower Monte Carlo programs: the POWHEG BOX, JHEP 1006 (2010) 43.

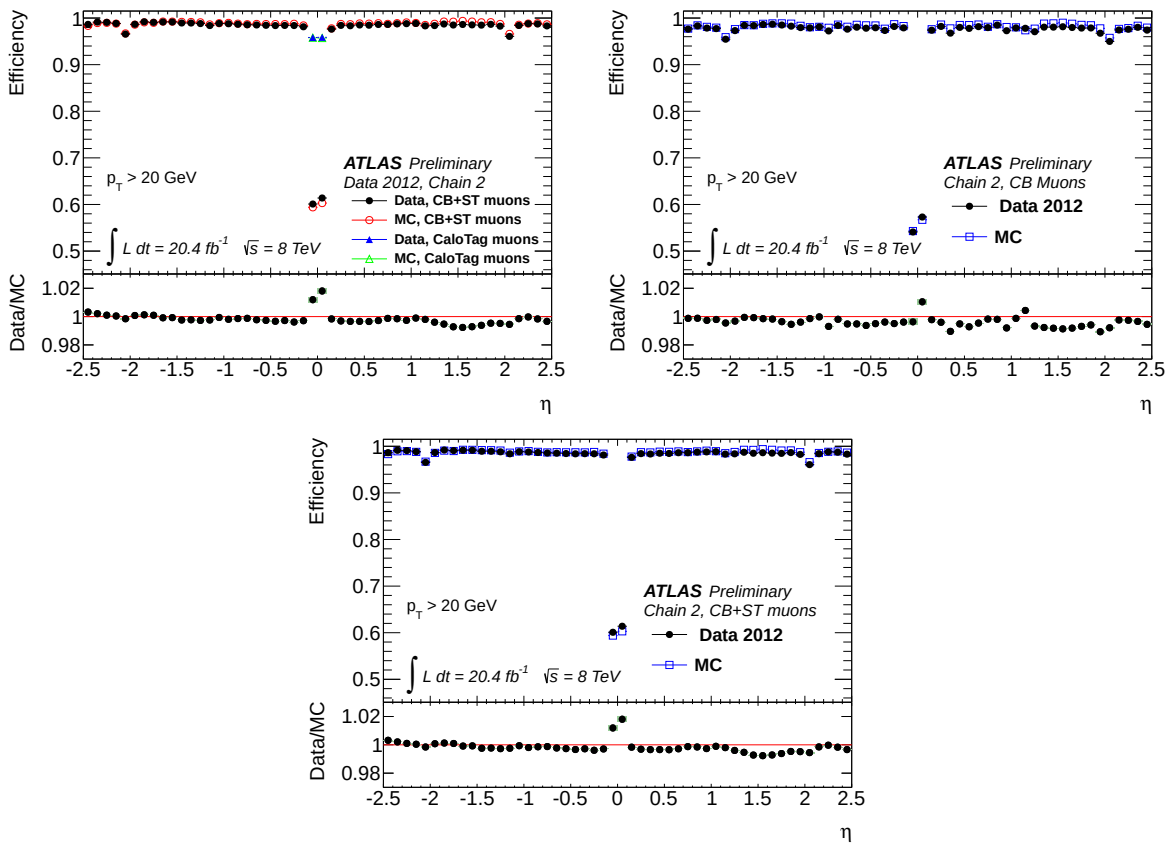

Figure 12: Muon reconstruction efficiency as a function of η for muons with $p_{\mathrm{T}} > 20$ GeV for various combinations of muon reconstruction types. CB and ST muon types are reconstructed using the Chain 2 reconstruction algorithm. The panel at the bottom of each insert shows the ratio between the measured and predicted efficiencies. The top left plot shows the reconstruction efficiency obtained by combining all the available muon reconstruction types (CaloTag muons are used only in the region $|\eta| < 0.1$). The top right plot shows the CB muon reconstruction efficiency. The bottom plot shows the CB+ST muon reconstruction efficiency.

[10] GEANT4 Collaboration, S. Agostinelli et al., Nucl.Instrum.Meth. A506 (2003) 250303.

[11] ATLAS Collaboration, Studies of the performance of the ATLAS detector using cosmic-ray muons, Eur. Phys. J. (2011), arXiv:1011.6665 [hep-ex].

[12] ATLAS Collaboration, Update on muon alignment for Rel 17, ATLAS-PLOT-MUON-2011-003 `https://cds.cern.ch/record/1383415`

[13] ATLAS Collaboration, Determination of the muon reconstruction efficiency in ATLAS at the Z resonance in proton-proton collisions at $\sqrt{s} = 7$ TeV, ATLAS-CONF-2011-008 (2011). `https://cds.cern.ch/record/1330715`

[14] ATLAS Collaboration, A measurement of the muon reconstruction efficiency in 2010 ATLAS data using J/ψ decays, ATLAS-CONF-2012-125 (2012). `https://cds.cern.ch/record/1474642`

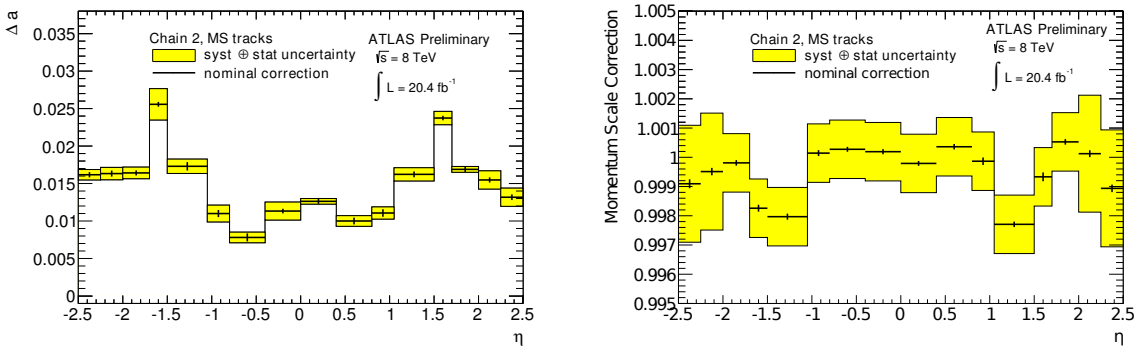

Figure 13: Resolution and scale MC correction terms for Chain 2 muon reconstruction algorithm derived from $Z \to \mu\mu$ events. The systematic uncertainty on the correction is shown in yellow. The left plot shows the Δa resolution correction term for the MS. The right plot shows the MS momentum scale correction.

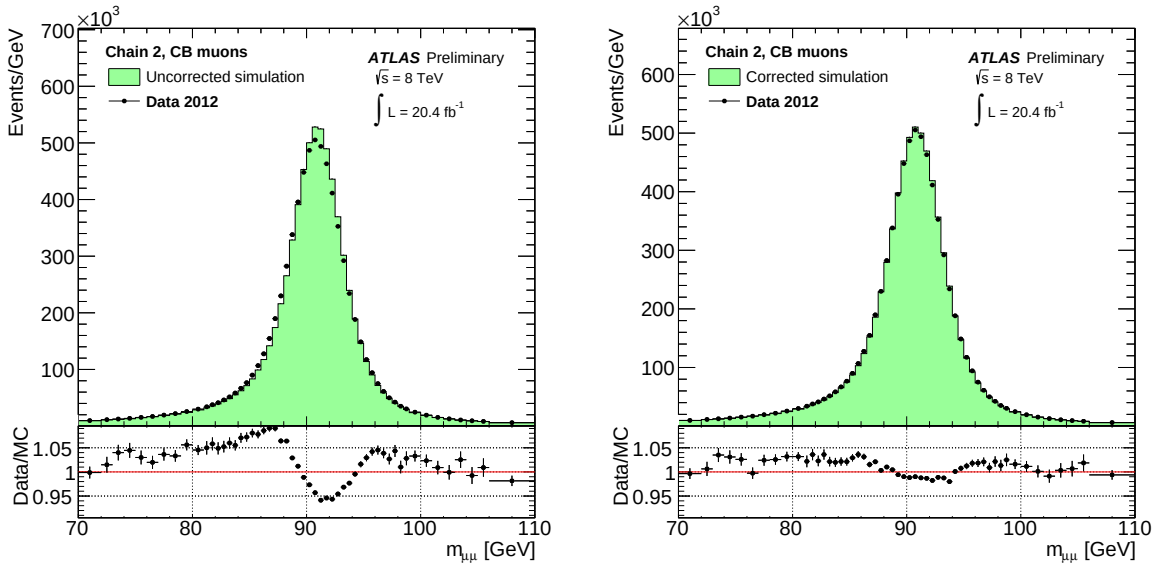

Figure 14: Di-muon invariant mass for Chain 2, CB muons, isolated and with $p_{\mathrm{T}} > 25$ GeV. The plot shows the invariant mass for 2012 data and for the POWHEG [9] simulation of $Z \to \mu\mu$ plus background events. No corrections are applied on the left plot while smearing and scale corrections are applied to the plot on the right. The corrections have been derived from the full 2012 dataset.

[15] ATLAS Collaboration, Performance of the ATLAS Inner Detector Track and Vertex Reconstruction in the High Pile-Up LHC Environment, ATLAS-CONF-2012-042 (2012). https://cds.cern.ch/record/1435196

[16] ATLAS Collaboration, J/ψ Performance of the ATLAS Inner Detector, ATLAS-CONF-2010-078 (2010). https://cds.cern.ch/record/1281369

[17] ATLAS Collaboration, Alignment of the ATLAS Inner Detector Tracking System with 2010 LHC proton-proton collisions at $\sqrt{s} = 7$ TeV, ATLAS-CONF-2011-012 (2011). https://cds.cern.ch/record/1334582